HHS Public Access

Author manuscript

Nature. Author manuscript; available in PMC 2015 October 19.

Published in final edited form as:

Nature. 2014 July 17; 511(7509): 358–361. doi:10.1038/nature13465.

WNT7A and PAX6 define corneal epithelium homeostasis and pathogenesis

Hong Ouyang[1,2], **Yuanchao Xue**[3], **Ying Lin**[1,2], **Xiaohui Zhang**[2,†], **Lei Xi**[1,2], **Sherrina Patel**[2], **Huimin Cai**[4,5], **Jing Luo**[2], **Meixia Zhang**[4], **Ming Zhang**[4], **Yang Yang**[2,†], **Gen Li**[4], **Hairi Li**[3], **Wei Jiang**[4], **Emily Yeh**[2], **Jonathan Lin**[2], **Michelle Pei**[2], **Jin Zhu**[2], **Guiqun Cao**[4], **Liangfang Zhang**[2,6], **Benjamin Yu**[7,8], **Shaochen Chen**[2,6], **Xiang-Dong Fu**[2,3,8], **Yizhi Liu**[1], and **Kang Zhang**[1,2,4,8,9]

[1]State Key Laboratory of Ophthalmology, Zhongshan Ophthalmic Center, Sun Yat-sen University, Guangzhou 510060, China

[2]Department of Ophthalmology, and Biomaterial and Tissue Engineering Center of Institute of Engineering in Medicine, University of California San Diego, La Jolla, California 92093, USA

[3]Department of Cellular and Molecular Medicine, University of California San Diego, La Jolla, California 92093, USA

[4]Molecular Medicine Research Center, State Key Laboratory of Biotherapy, West China Hospital, Sichuan University, Sichuan 610041, China

[5]Guangzhou KangRui Biological Pharmaceutical Technology Company Ltd., Guangzhou 510005, China

[6]Department of Nanoengineering, University of California San Diego, La Jolla, California 92093, USA

[7]Department of Medicine, University of California San Diego, La Jolla, California 92093, USA

[8]Institute for Genomic Medicine, University of California San Diego, La Jolla, California 92093, USA

[9]Veterans Administration Healthcare System, San Diego, California 92093, USA

Abstract

Correspondence and requests for materials should be addressed to: K.Z. (kangzhang@ucsd.edu), X.-D.F. (xdfu@ucsd.edu) or Y.Z.L. (yzliu62@yahoo.com).

[†]Present addresses: Beijing Institute of Ophthalmology, Beijing Tongren Eye Center, Beijing 100730, China (X.Z.); Department of Ophthalmology, Shengjing Hospital of China Medical University, Shenyang 110004, China (Y.Y.).

Author Contributions H.O., X.-D.F., Yiz. L., and K.Z. designed study, interpreted data and wrote the manuscript. H.O., Y.X., Yin. L., X.Z., L.X., H.C., J.L., Mei. Z., Min. Z., Y.Y., H.L., G.L., E.Y., G.C., J.Z. and B.Y. performed the experiments. Y.L., W.J., J.L. and Yiz. L. obtained human samples. S.C., S.P., M.P. and L.Z. contributed to data analysis and interpretation.

Microarray and RNA sequence information has been submitted to the Gene Expression Omnibus database under accession number GSE32145 and GSE54322.

The authors declare no competing financial interests.

Readers are welcome to comment on the online version of the paper.

The surface of the cornea consists of a unique type of non-keratinized epithelial cells arranged in an orderly fashion, and this is essential for vision by maintaining transparency for light transmission. Cornea epithelial cells (CECs) undergo continuous renewal from limbal stem or progenitor cells (LSCs)[1,2], and deficiency in LSCs or corneal epithelium—which turns cornea into a non-transparent, keratinized skin-like epithelium—causes corneal surface disease that leads to blindness in millions of people worldwide[3]. How LSCs are maintained and differentiated into corneal epithelium in healthy individuals and which key molecular events are defective in patients have been largely unknown. Here we report establishment of an *in vitro* feeder-cell-free LSC expansion and three-dimensional corneal differentiation protocol in which we found that the transcription factors p63 (tumour protein 63) and PAX6 (paired box protein PAX6) act together to specify LSCs, and WNT7A controls corneal epithelium differentiation through PAX6. Loss of WNT7A or PAX6 induces LSCs into skin-like epithelium, a critical defect tightly linked to common human corneal diseases. Notably, transduction of PAX6 in skin epithelial stem cells is sufficient to convert them to LSC-like cells, and upon transplantation onto eyes in a rabbit corneal injury model, these reprogrammed cells are able to replenish CECs and repair damaged corneal surface. These findings suggest a central role of the WNT7A–PAX6 axis in corneal epithelial cell fate determination, and point to a new strategy for treating corneal surface diseases.

Corneal and skin epithelium share many similarities, including a typical morphology of stratified epithelium and maintenance of their stem cells by p63 in the keratin 5/keratin 14^{+} (K5/K14)-expressing basal cell layer in limbus and epidermis[4–8] (Fig. 1a, b and Extended Data Fig. 1a, b). However, there are marked differences between them. Skin epithelial stem cells (SESCs) move upwards from a deep to suprabasal layers vertically during differentiation[9,10], where K5 and K14 are replaced by skin-specific K1 and K10 (ref. 11 and Extended Data Fig. 1c, d). In contrast, LSCs (defined by K19 at the limbus[12], see Fig. 1a and Extended Data Fig. 1e) migrate centripetally for several millimetres to the central cornea during which it undergoes differentiation and K5/K14 are replaced by corneal-specific K3 and K12 (refs 13, 14, Fig. 1c and Extended Data Fig. 1f).

A clear, transparent cornea maintained by CECs is essential for vision. Pathological conversion of CECs into skin-like epithelial cells, as indicated by morphological changes and switches in keratin expression (for example, replacement of cornea-specific K3 and K12 by skin-specific K1 and K10 along with K5^{+} cells at the basal layer; see Fig. 1d), leads to the loss of transparency in the cornea and causes millions of people around the world to suffer from partial or complete blindness[3], but the underlying mechanism has remained largely unknown.

To elucidate potential disease mechanisms, we successfully developed a feeder-free cell culture protocol to expand LSCs from human donors, enabling us to generate a homogeneous cell population to delineate key factors involved in controlling LSC cell fate determination and CEC differentiation. Proliferating LSCs were characterized by positive p63 and K19 with a high percentage of mitotic marker Ki67 (Fig. 2a and Extended Data Fig. 1g). We next established a three-dimensional LSC differentiation protocol to establish a three-dimensional CEC sphere structure from a single LSC within 14 to 18 days, as evidenced by strong expression of the CEC-specific markers K3 and K12 (Fig. 2b). The

three-dimensional differentiation sphere was further characterized by key differences in gene expression between LSCs and CECs; the latter showed increased expression of *K3* (31.2-fold higher) and *K12* (24.7-fold higher) and concomitant decreased expression of *K19* (6.2-fold lower, all $P < 0.01$; see Extended Data Fig. 1h). We took a similar strategy to expand SESCs and observed strong expression of typical SESC markers p63 and K5 in cultured SESCs (Fig. 2c). As expected, we detected increased expression of epidermal differentiation markers *K1* (16.6-fold higher) and *K10* (225.8-fold higher) in three-dimensional differentiated skin epithelial cells (SECs) compared to SESCs (Fig. 2d, Extended Data Fig. 1i, j).

To identify additional genes uniquely expressed in LSCs, CECs and SESCs, we performed genome-wide gene expression analysis (Fig. 2e and Extended Data Fig. 2a, b). Among genes that were differentially expressed, we focused on signalling molecules and transcription factors because of their central roles in cell fate determination and differentiation. We identified that *WNT7A* and *PAX6* were highly expressed in LSCs and CECs when compared to SESCs (*PAX6*, 8.8-fold higher in LSCs and 12.3-fold higher in CECs, $P < 0.001$; *WNT7A*, 4.5-fold higher in LSCs, 6.0-fold higher in CECs, $P < 0.001$) (Fig. 2e and Extended Data Fig. 2c). We observed that WNT7A expression precisely mirrored the expression pattern of PAX6 in *in vitro* LSC and CEC cultures, and in *in vivo* epithelial layers of cornea and limbus from infant to adult, while both of these genes were undetectable in skin epidermis (Fig. 2f and Extended Data Fig. 2d).

To determine the clinical relevance of WNT7A and PAX6 expression in LSCs and CECs, we examined several types of human corneal diseases, corneal epithelium squamous metaplasia, inflammatory keratopathy, trauma and alkaline burn. We observed the localized expression of p63 and K5 at the basal layer (Fig. 3a and Extended Data Fig. 3), and the expression of K10 in the suprabasal layer (Fig. 1d and Extended Data Fig. 3). We also found that WNT7A and PAX6 expression, and K3 and K12 expression were conspicuously absent in areas of metaplasia, while they were positive in surrounding corneal epithelium (Fig. 3a and Extended Data Fig. 3). These results suggest cornea epithelial cells were switched to skin-like epithelial cells in patient tissues with these disease conditions.

Wnt molecules are secreted signalling proteins that have a critical role in controlling cell fate decisions and tissue specification[15]. PAX6 is also a well-known control gene for eye development and disease[16]. However, it has remained unclear whether the loss of PAX6 is the cause or the consequence of abnormal skin epidermal differentiation in ocular surface diseases.

To demonstrate that WNT7A and PAX6 are necessary for LSC and CEC cell fate determination and differentiation, we used lentiviral short hairpin RNAs (shRNAs) to knock them down specifically in LSCs. Although LSCs with knockdown of either *WNT7A* or *PAX6* did not change proliferation and morphological properties (Extended Data Fig. 4a), these treatments significantly diminished the expression of corneal K3 and K12 under the three-dimensional differentiation conditions (*WNT7A* knockdown: 24.7-fold lower in *K3*, 22.6-fold lower in *K12; PAX6* knockdown: 20.8-fold lower in *K3*, 21.4-fold lower in *K12*; all $P < 0.05$), and concurrently, the expression of skin-specific K1 and K10 became more

prominent (*WNT7A* knockdown: 3.9-fold higher in *K1* and 5.7-fold higher in *K10; PAX6* knockdown: 3.1-fold higher *K1* and 6.1-fold higher in *K10*; all $P < 0.05$), indicative of more skin-like differentiation (Fig. 3b, c). Moreover, knockdown of *WNT7A* reduced *PAX6* expression in LSCs (1.8-fold lower, $P < 0.001$); this repressive effect was even stronger in differentiated CECs (8.0-fold lower, $P < 0.01$). In contrast, there was no significant difference in *WNT7A* expression when *PAX6* was knocked down in either LSCs or CECs (Fig. 3c and Extended Data Fig. 4b, c). These results suggest that WNT7A acts upstream of PAX6 during CEC differentiation.

To study further the role of the Wnt signalling pathway in corneal fate determination and differentiation, we investigated the functional requirement of Frizzled receptors, which have been shown to interact and transduce WNT7A signalling based on co-immunoprecipitation[17]. We found that WNT7A interacted strongly with Frizzled 5 (FZD5) in LSCs (Extended Data Fig. 4d, e), and as predicted, knockdown of *FZD5* in LSCs also led to reduced *PAX6* expression (1.7-fold lower in LSCs and 3.0-fold lower in differentiated CECs ($P < 0.001$) (Extended Data Fig. 4f). Together, these data demonstrated that loss of WNT7A or PAX6 led to a switch of corneal epithelial cells to skin-like epidermal cells and that WNT7A and FZD5 acted as the upstream regulators of PAX6 expression in corneal differentiation.

Given the central role of PAX6 in eye development[16], we next tested the possibility that engineered expression of PAX6 might be able to convert SESCs into LSC-like cells (Extended Data Fig. 5a). Indeed, we found that the expression of either PAX6a or PAX6b in SESCs was sufficient to convert them into LSC-like cells, as evidenced by the induced K19 expression on the surface, coincident with the expression of both p63 and PAX6 in the nucleus (Fig. 4a). When placed in three-dimensional culture, *PAX6*-transduced SESCs showed dramatic increase in corneal K3 and K12 expression (9.4-fold higher and 72.7-fold higher, all $P < 0.05$) with concomitant decrease in skin K1 and K10 expression (20.8-fold lower and 20.0-fold lower, all $P < 0.01$) (Fig. 4b, c and Extended Data Fig. 5b, c). To obtain global evidence for successful cell fate conversion, we performed gene expression profiling by RNA sequencing (RNA-seq)[18] on CECs, SECs and LSCs after knocking down *PAX6* and on SESCs transduced with *PAX6* upon three-dimensional differentiation. We generated 3 to 7 million reads from each biological sample that were uniquely mapped to the RefSeq database (Extended Data Fig. 6a). Pairwise comparison demonstrated that the data were very reproducible within the same group of samples (Extended Data Fig. 6b); in contrast, when compared between cells with different fates, the data demonstrate remarkable differences based on the statistical cut-off of false discovery rate (FDR) < 0.001 (Extended Data Fig. 6c). We displayed the entire data sets that recorded the expression of >10,000 genes in various cell types (Fig. 4d), demonstrating that both induced (red) and repressed (green) genes were clearly co-segregated between CECs and $PAX6^+$ SESCs and between *PAX6* shRNA-treated LSCs and SECs. These data therefore provided global evidence for a role of the WNT7A–PAX6 axis in cell fate conversion from SESCs to CECs. Together, these data suggest that defects in the WNT7A–PAX6 axis are likely to be responsible for metaplastic conversion of corneal cells to skin epidermal-like cells in corneal diseases in humans (shown

in Fig. 4e), although further studies need to be performed to determine the significance of the WNT7 and PAX6 axis in corneal epithelial differentiation.

Finally, we tested the treatment and repair potential of SESCs with engineered expression of PAX6 (Extended Data Fig. 7a–c) for corneal epithelial defects in a rabbit LSC deficiency model (Extended Data Fig. 7f), which mimics a common corneal disease condition in humans. We showed that rabbit SESCs with PAX6 transduction formed a continuous sheet of epithelial cells with positive staining of corneal-specific K3 and K12 (Fig. 5a) and successfully repaired epithelium defect of the entire corneal surface to restore and maintain normal cornea clarity and transparency for over 3 months (Fig. 5b–g and Extended Data Fig. 8). By following the time course of corneal epithelial surface repair using GFP-labelled $PAX6^+$ SESCs, we observed that these PAX6-reprogrammed SESCs were initially only located at the limbal region and then moved progressively towards the central cornea with corresponding areas of restored cornea clarity (Extended Data Fig. 9a). Importantly, these grafted cells were indeed able to repopulate limbus as evidenced by culture and re-isolation of $PAX6^+$ SESCs from limbal region (Extended Data Fig. 9b). Notably, these reprogrammed SESCs were capable of repairing large corneal epithelium defects after repeated corneal epithelial scraping (Extended Data Fig. 9c). In marked contrast, transplanting rabbit LSCs with *PAX6* knockdown (Extended Data Fig. 7a, d, e) onto denuded corneal surface resulted in a $K10^+$ skin-like epithelium with opacity and vascularization (Fig. 5f). Together, these data demonstrate that SESCs with PAX6 expression are able to trans-differentiate into corneal-like epithelium and repair corneal surface defects.

In summary, this work establishes the feasibility of expanding LSCs under feeder-free conditions and its therapeutic potential, and demonstrates key roles of WNT7A and PAX6 in corneal lineage specification. Importantly, SESCs or other cell types converted into a corneal fate by PAX6 expression may serve as a potential source for corneal surface repair and regeneration, particularly in patients with total LSC deficiency. This would overcome a major feasibility problem in using a patient's own reprogrammed LSCs for transplantation, thus pointing to a potential therapeutic strategy for treating many common corneal diseases in humans.

METHODS SUMMARY

LSCs and SESCs were isolated from rabbits and human donors in feeder-free media and differentiated in the three-dimensional culture conditions. Histology, immunohistochemistry and immunocytochemistry were carried out on paraffin sections as well as on cultured cells. Gene expression microarray, RNA-seq and quantitative PCR (qPCR) were performed using total RNA isolated from LSCs, SESCs and CECs. Lentiviral RNA interference and engineered-expression study of WNT7A, PAX6 and FZD5 were carried out in LSCs and SESCs. Cell transplantation of LSCs and SESCs was performed on animal models of corneal injury. Detailed information is provided in the supplement.

Online Content Methods, along with any additional Extended Data display items and Source Data, are available in the online version of the paper; references unique to these sections appear only in the online paper.

Extended Data

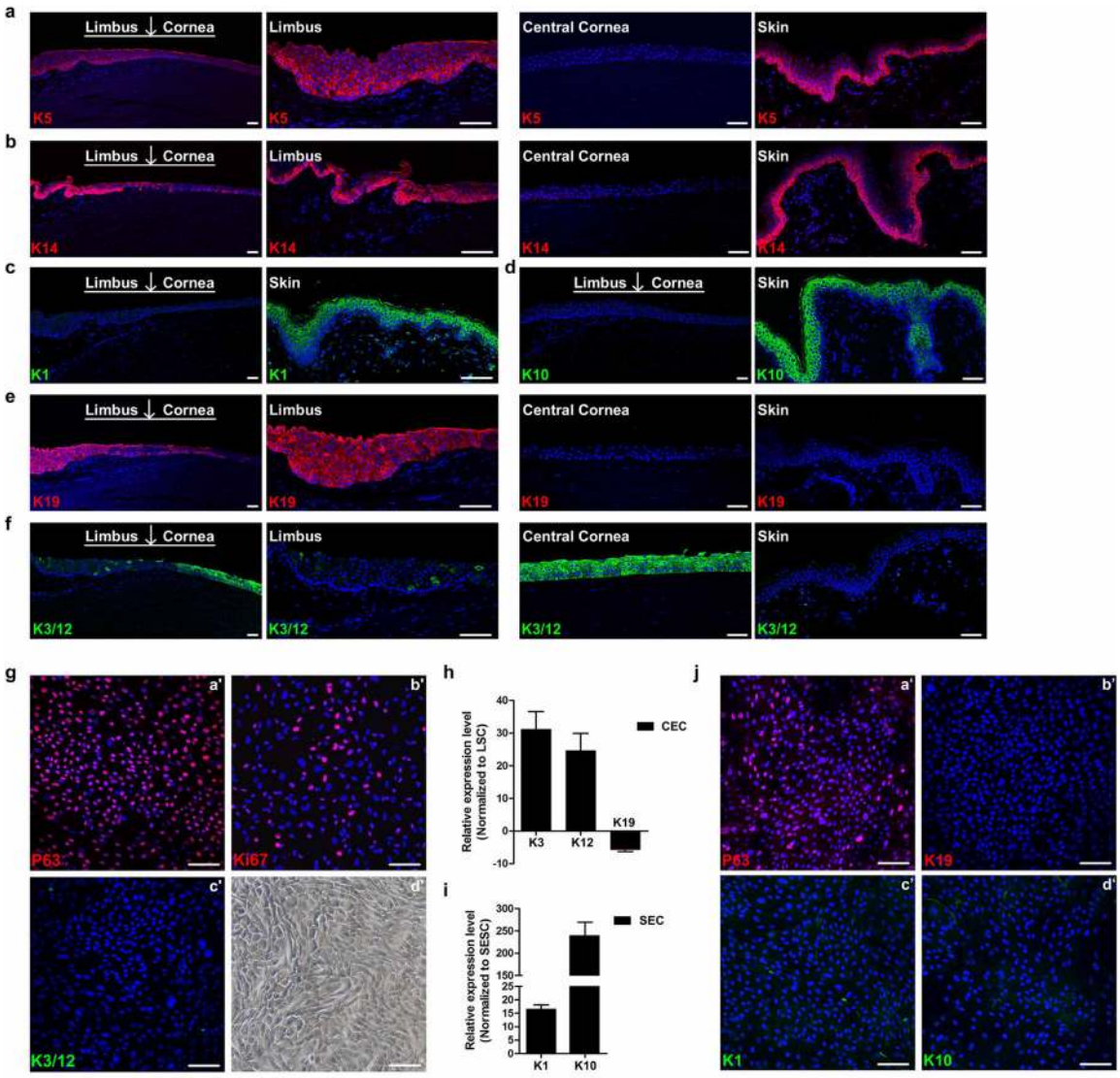

Extended Data Figure 1. Keratin expression profiles and cell cultures, and three-dimensional differentiation of LSCs and SESCs

a–f, Keratin expression profiles in human limbus, cornea and skin epidermis. **a**, **b**, Peripheral cornea–limbus junction and skin tissues showing K5$^+$ (**a**) and K14 (**b**) expression in the basal cell layer of limbus and skin, and their absence in central corneal epithelium. **c**, **d**, Skin epidermis showing positive K1 (**c**) and K10 (**d**) expression and their absence in cornea and limbus. **e**, **f**, Peripheral cornea–limbus junction showing K19$^+$ staining in limbus but not in central corneal epithelium and skin (**e**), and K3/12$^+$ staining only in cornea and not in limbus and skin (**f**). **g–j**, Cultured LSCs with stem and progenitor cell characteristics, and SESC characteristics at passage 12 and validation of a three-dimensional differentiation system. **g**, Immunofluorescence staining of LSCs showing positive stem cell signals of p63 (**a′**) and Ki67 (**b′**) and negative differentiated CEC signals, K3/12 (**c′**), phase contrast photograph (**d′**). **h**, qPCR analysis showing K3/12 upregulation and K19 downregulation in

CECs from a three-dimensional differentiation assay compared with LSCs. **i**, K1 and K10 upregulation in SECs from three-dimensional differentiation assay compared with SESCs (**c**), all $n = 3$, $P < 0.01$. **j**, Immunofluorescence staining of cultured SESCs showing positive p63 (**a′**) and negative signals for limbus stem cell marker, K19 (**b′**) and mature skin epithelium markers K1 and K10 (**c′**, **d′**). Scale bars, 100 μm. Data shown as means ± s.d.

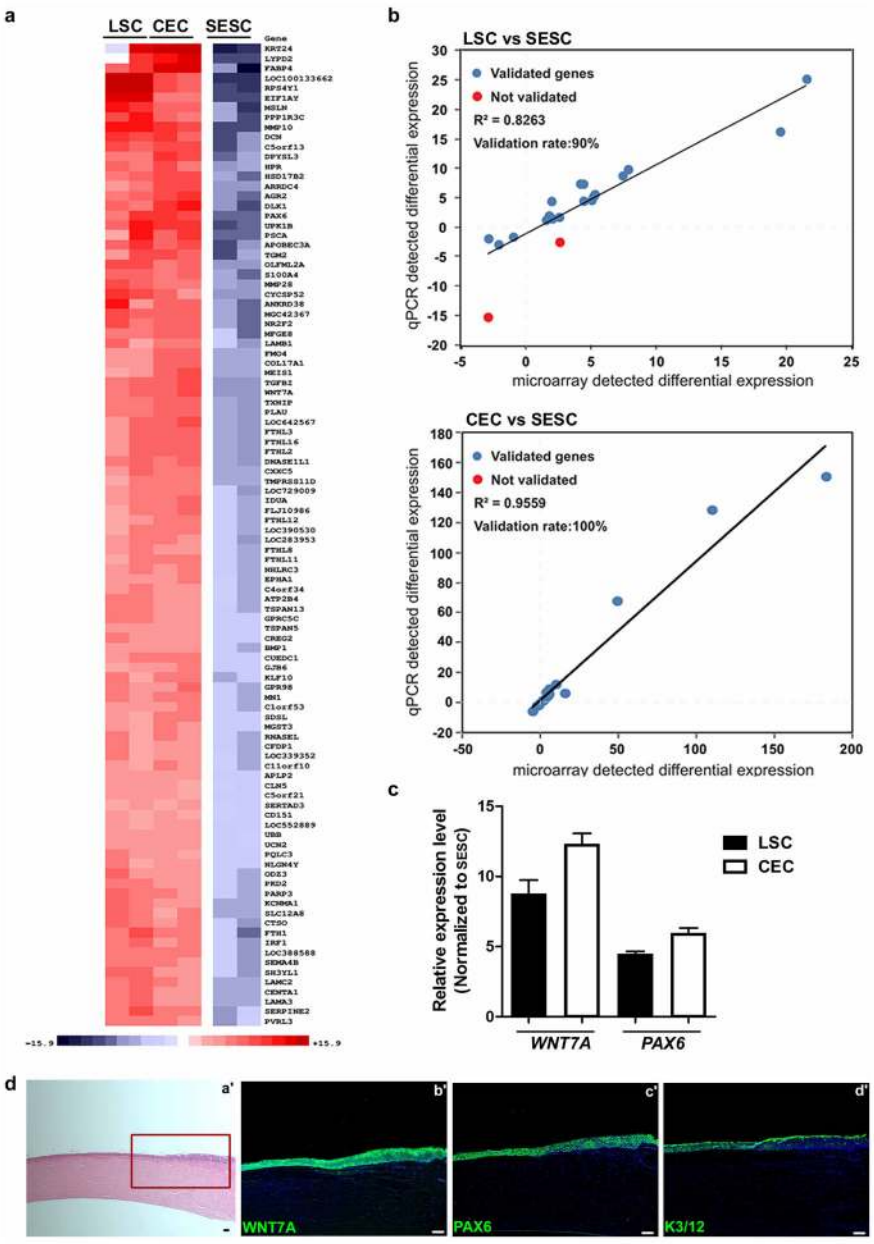

Extended Data Figure 2. Gene expression profiling and immunohistological analysis

a–c, Genome-wide gene expression microarray of LSCs, CECs and SESCs. **a**, The top 100 significant genes in a comparison of LSCs and CECs to SESCs. **b**, Validation of the microarray data with qPCR analysis showing a strong correlation. **c**, qPCR analysis of

WNT7A and *PAX6* expression in LSCs and CECs compared to SESCs, all $n = 3$, $P < 0.05$. **d**, Expression of WNT7A and PAX6 in cornea and limbus of a one-year old human infant. H&E stain (**a′**), boxed area was shown in serial sections (**b′–d′**) with immunofluorescence staining of WNT7A (**b′**), PAX6 (**c′**) and K3/12 (**d′**). All scale bars, 100 μm. Data shown as means ± s.d.

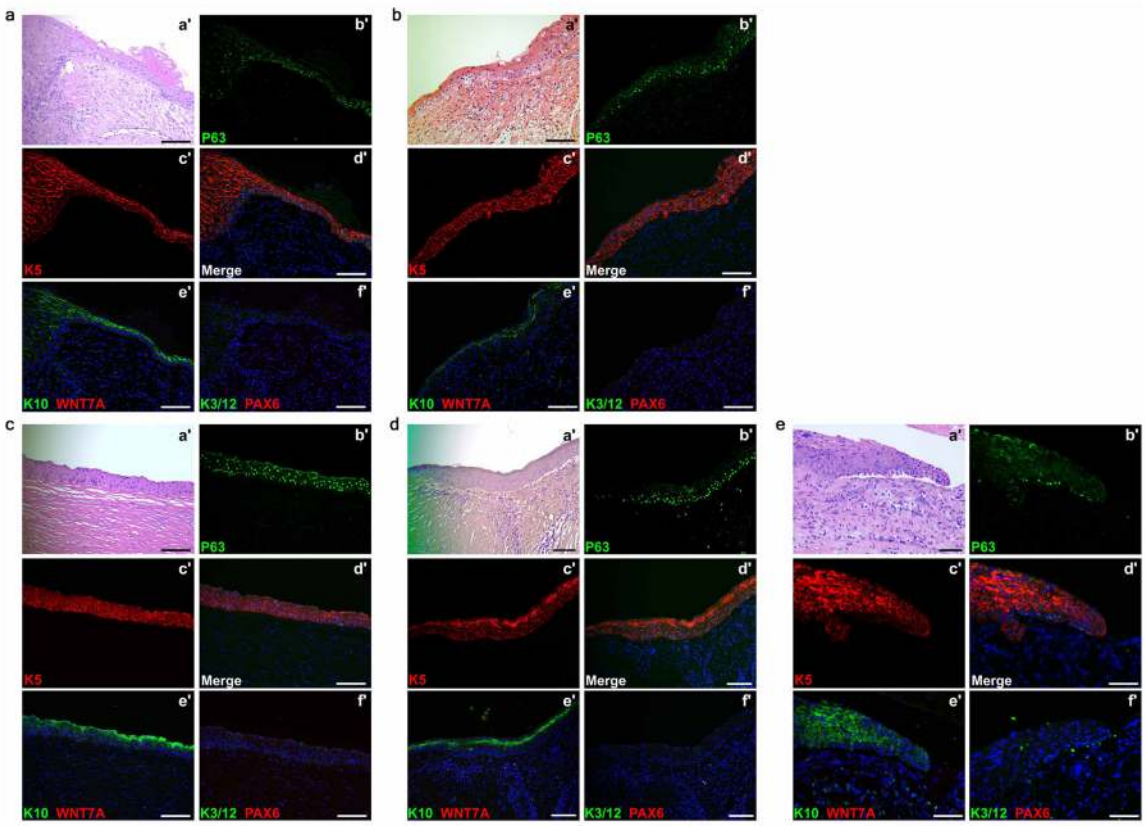

Extended Data Figure 3. Appearance of skin epidermal markers with loss of corneal markers in human corneal diseases

Appearance of skin epidermal markers p63, K5 and K10 with loss of corneal marker K3/12, PAX6 and WNT7A in cornea of patients with Stevens–Johnson syndrome (**a**, **b**), ocular pemphigoid (**c**), trauma injury (**d**) and alkaline burn (**e**). For all images, H&E staining was carried out on the lesion of corneal epithelial squamous metaplasia (**a′**). **b′–f′**, the same region of lesion in serial sections showing increased p63 (**b′**, **d′**) and K5 (**c′**, **d′**) and K10 (**e′**) in the suprabasal layer, no WNT7A (**e′**), K3/12 or PAX6 could be detected in the area (**f′**). Scale bars, 100 μm.

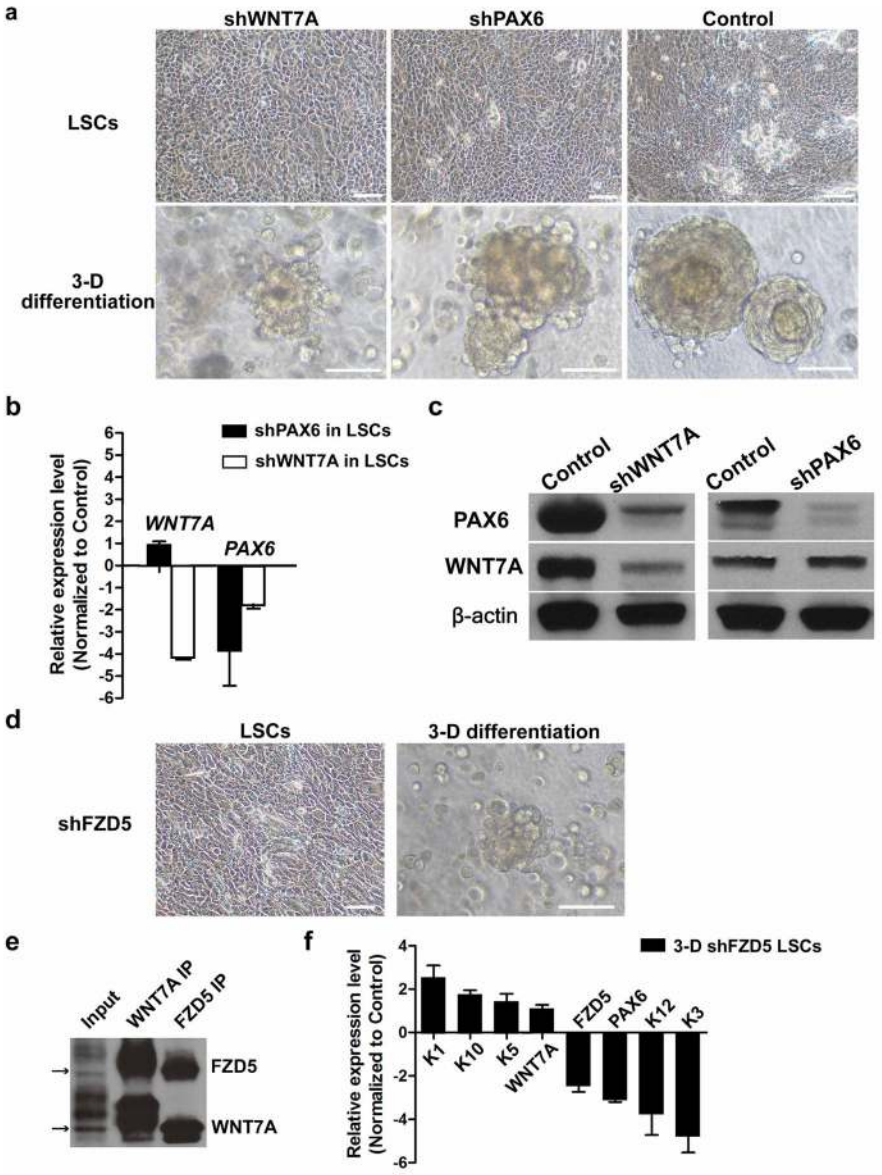

Extended Data Figure 4. The effect of *WNT7A* and *FZD5* on *PAX6* expression in LSCs

a–c, The effect of *WNT7A* knockdown on *PAX6* expression in LSCs. **a**, Phase contrast photographs showing effects of *WNT7A* and *PAX6* knockdowns (shWNT7A and shPAX6) in LSCs and their three-dimensional differentiation spheres. **b**, qPCR analysis of gene expression changes of *WNT7A* and *PAX6* in LSCs. *WNT7A* knockdown decreased *PAX6* expression ($n = 3$, $P < 0.01$); no significant change in *WNT7A* expression in *PAX6* knockdown. **c**, Validation of knockdown efficiency of WNT7A and PAX6 in LSCs by western blot analysis. **d–f**, WNT7A and FZD5 acted as the upstream regulators of PAX6 expression. **d**, Phase contrast photographs showing cell morphology of knockdown of *FZD5* (shFZD5) in LSCs and three-dimensional differentiation spheres. **e**, Co-immunoprecipitation of WNT7A and FZD5 in LSCs. **f**, qPCR analysis of gene expression changes in corneal and skin epithelial markers in three-dimensional differentiated cells of LSCs with *FZD5*

knockdown (three-dimensional shFZD5 LSCs). *FZD5* knockdown did not affect *WNT7A* expression; all others, $n = 3$, $P < 0.05$. Scale bars, 100 μm. Data shown as means ± s.d.

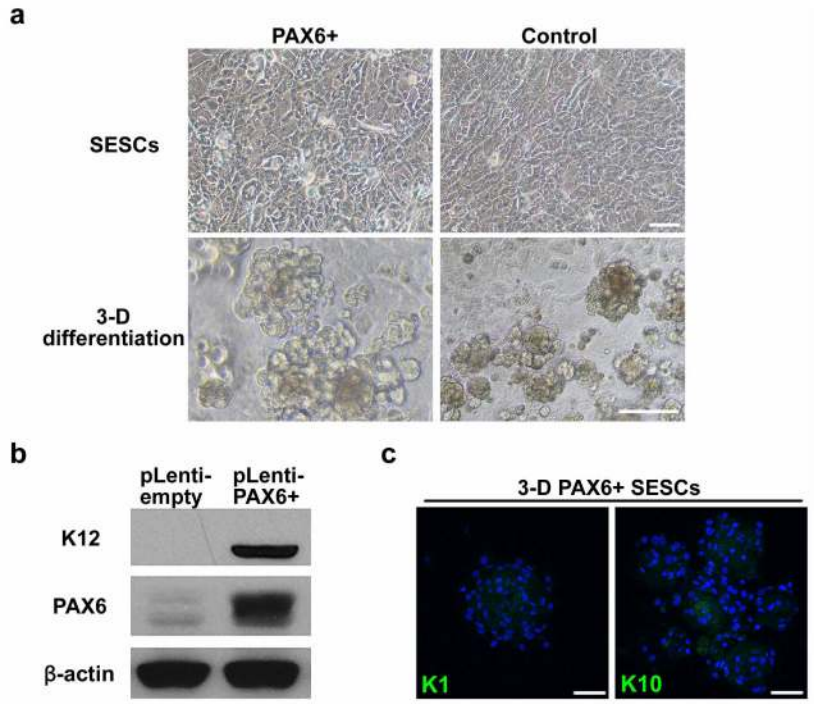

Extended Data Figure 5. The effect of *PAX6* transduction in SESCs

a, Phase contrast photographs of SESCs with *PAX6* transduction (PAX6$^+$) and three-dimensional differentiation spheres. **b**, Validation of K12 and PAX6 expression in three-dimensional differentiation spheres by western blotting analysis. **c**, Loss of skin-specific keratins, K1 and K10 in three-dimensional differentiation of SESCs with *PAX6* transduction (three-dimensional PAX6$^+$ SESCs). Scale bars, 100 μm.

a

Sample	Raw Reads	Mapping Reads	Mapping Rate
CEC-1	4831619	3221767	0.667
CEC-2	4926847	3089309	0.627
SEC-1	4590757	2776526	0.605
SEC-2	11971991	7073156	0.591
3-D shPAX6 LSC-1	8946779	5345343	0.597
3-D shPAX6 LSC-2	7370502	4462113	0.605
3-D PAX6+SESC-1	6872086	4594613	0.669
3-D PAX6+SESC-2	6347059	4191302	0.660

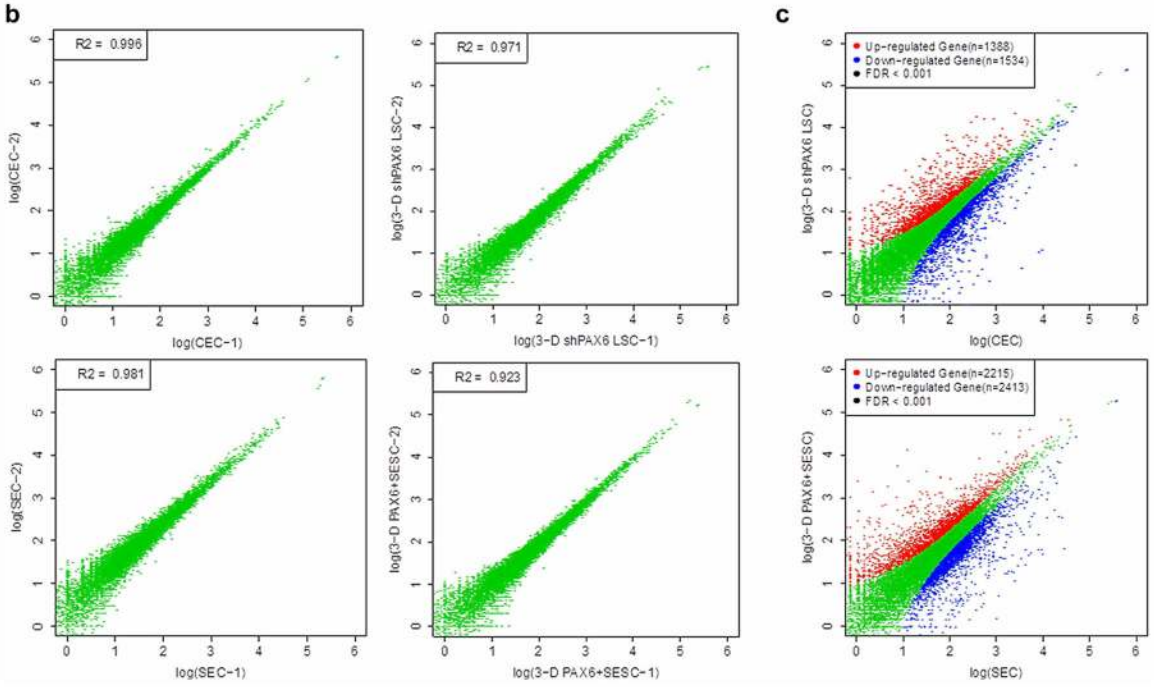

Extended Data Figure 6. Quantitative information from RNA-seq data

a, Statistical analysis of RNA-seq samples: raw reads, mapping reads and mapping rate of each sample are included. **b**, Pairwise comparisions of duplicated biological samples. **c**, The differences between SECs and three-dimensional PAX6$^+$ SESCs, CECs and three-dimensional shPAX6 LSCs, all FDR < 0.001. **a**, qPCR analysis of PAX6 expression in rabbit SESCs with PAX6 transduction (rabbit (Rb) PAX6$^+$ SESCs) or LSCs with PAX6 knockdown (Rb shPAX6 LSCs) (all $n = 3$, $P < 0.05$). We noticed some minor differences in the heatmap. These might result from some experimental variations, or it is possible that, although PAX6 expression is largely responsible for cell fate switch from SESCs to CECs at gene expression and functional levels (as demonstrated in this study), this single transcription factor may not be sufficient to create cells that are completely identical to CECs.

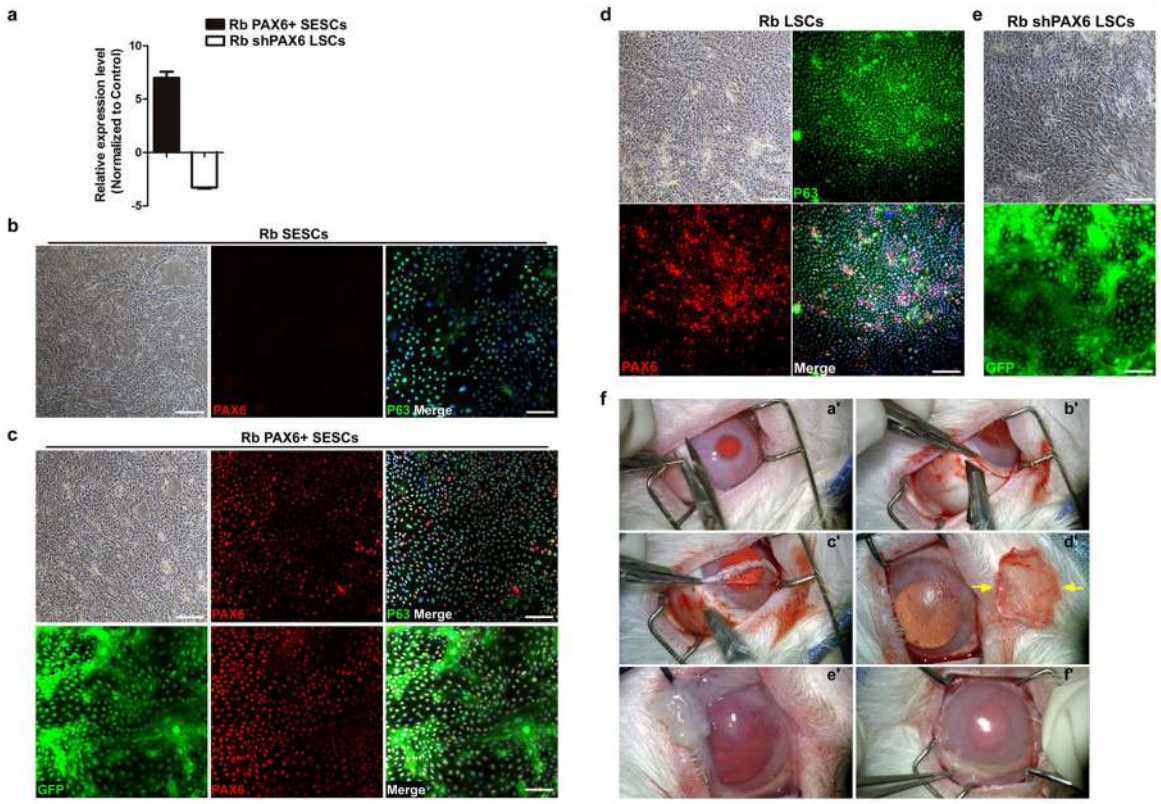

Extended Data Figure 7. Engineered expression of PAX6 and rabbit LSC deficiency model

a–e, Quantification and culture of engineered expression of PAX6 in rabbit SESCs and PAX6 knockdown LSCs. **a**, qPCR analysis of PAX6 expression in rabbit SESCs with PAX6 transduction (Rb PAX6$^+$ SESCs) or LSCs with PAX6 knockdown (Rb shPAX6 LSCs) (all $n = 3$, $P < 0.05$). **b**, Rabbit SESCs with positive staining of p63 and negative staining of PAX6. Left panel, phase contrast photograph. **c**, Top row, double immunofluorescence staining of PAX6 and p63 in rabbit SESCs with PAX6 transduction. Top left panel, phase contrast photograph. Bottom row, rabbit PAX6$^+$ SESCs were further labelled with GFP for transplantation. **d**, Rabbit LSCs with positive staining of p63 and PAX6. Top left panel, phase contrast photograph. **e**, Culture of GFP-labelled rabbit LSCs with *PAX6* knockdown. **f**, conjunctiva peritomy was performed and a circumferential strip of 2mm anterior limbal conjunctiva was removed (**a′**). Lamellar scleral and corneal dissection to completely remove LSCs and corneal epithelium along an anterior cornea stroma plane (**b′–d′**). Dissected cap is shown in (**d′**, arrows). The exposed cornea stroma bed was covered by human amniotic membrane (**e′**) and sutures (**f′**). ($n = 3$). Scale bars, 100 μm. Data shown as means ± s.d.

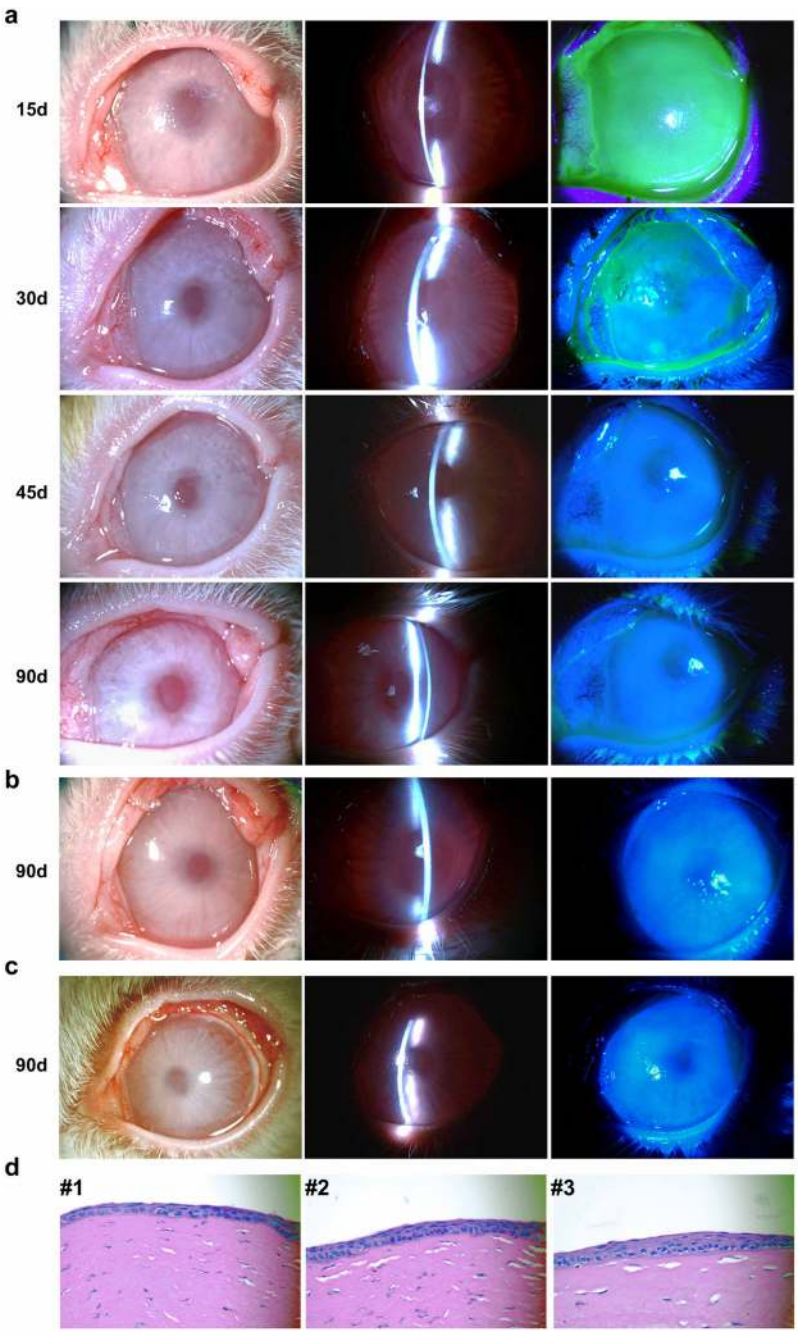

Extended Data Figure 8. Cornea epithelium regeneration and repair by transplanted GFP-labelled PAX6^{+} SESCs in a rabbit LSC deficiency model

a, Time course of corneal epithelial defect repair. Fifteen days post transplantation, there was decreased cornea clarity with an entire corneal epithelial defect evidenced by fluorescein stain of cornea surface; 30 days post transplantation there was improved cornea clarity and reduced fluorescein staining of cornea epithelial defect; 45 and 90 days post transplantation there was restoration and maintenance of cornea clarity. **b**, **c**, Two other examples of regeneration and repair of rabbit corneal epithelial surface 90 days post

transplantation with GFP-labelled PAX6$^+$ SESCs showing complete repair and re-epithelization of corneal epithelial defects. Left panels, white light micrographs; middle panels, slit-lamp micrographs; right panels, fluorescein staining (note that bright spots on the corneal surface were due to camera light reflection, they were not epithelial defects) of corneal epithelium (n = 5). **d**, H&E stain of regeneration and repair of corneal epithelial surface in three separate rabbits 90 days post transplantation with GFP-labelled PAX6$^+$ SESCs showing intact corneal epithelium histology.

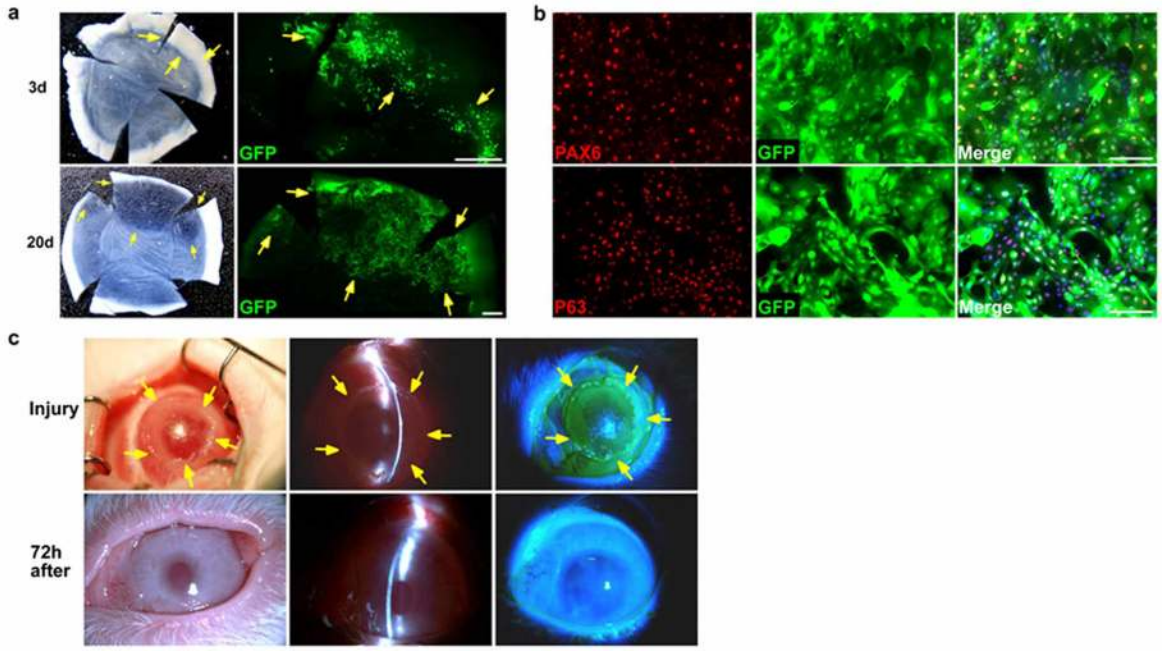

Extended Data Figure 9. Corneal epithelial regeneration by transplantation in a rabbit LSC deficiency model

a, Time course of corneal epithelial regeneration and repair in a rabbit LSC deficiency model post transplantation with GFP-labelled PAX6$^+$ SESCs. Top panels, 3 day post transplantation. left, light micrograph showing a hazy cornea; right, GFP+ donor cells at limbal region (arrows). Bottom panels, 20 days post transplantation. Left, light micrograph showing a cornea with partial clarity; right, GFP$^+$ donor co-located in transparent areas (arrows). Scale bars, 1 mm. We observed that only the transplanted cells from the limbal region could survive, proliferate and regenerate cornea surface epithelium, suggesting that limbus contained the stem cell niche favourable for stem cell survival and growth. **b**, Culture and re-isolation of reprogrammed donor GFP-labelled PAX6$^+$ SESCs epithelial cells from the limbal region of a rabbit recipient eye 90 days post transplantation with GFP-labelled PAX6$^+$ SESCs. Top panel, double immunofluorescence staining of PAX6 and GFP; bottom panel, double immunofluorescence staining of p63 and GFP in *PAX6*-transduced rabbit SESCs. Scale bars, 100 μm. **c**, Repair and recovery of a repeat cornea epithelium injury on a cornea transplanted with GFP-labelled PAX6$^+$ SESCs. Top panels, we iatrogenically scraped and removed donor-derived corneal epithelial cells and made a large corneal surface epithelium defect (arrows) 3 months post initial transplantation of PAX6$^+$ SESCs. Bottom panels, complete repair and recovery were observed within 72 h with healed epithelial defect

(n = 3). Left panels, light micrographs; middle panels, slit-lamp micrographs; right panels, fluorescein staining.

Extended Data Table 1

Primer sequences and rabbit transplantation results

Extended Data Table 1a. Primer sequences

Gene (Human)	Forward Primer	Reverse Primer
CASZ1	*GTTCTACGGACAGAAGACCACG*	*TCTTGAAGCCGTCCTTGGCGTA*
FGFR3	*AGTGGAGCCTGGTCATGGAA*	*GGATGCTGCCAAACTTGTTCTC*
FZD5	*TGGAACGCTTCCGCTATCCTGA*	*GGTCTCGTAGTGGATGTGGTTG*
GAPDH	*GAGTCAACGGATTTGGTCGT*	*GACAAGCTTCCCGTTCTCAG*
ID2	*TTGTCAGCCTGCATCACCAGAG*	*AGCCACACAGTGCTTTGCTGTC*
K1	*CAGCATCATTGCTGAGGTCAAGG*	*CATGTCTGCCAGCAGTGATCTG*
K3	*ACGTGACTACCAGGAGCTGATG*	*ATGCTGACAGCACTCGGACACT*
K5	*GCTGCCTACATGAACAAGGTGG*	*ATGGAGAGGACCACTGAGGTGT*
K10	*CCTGCTTCAGATCGACAATGCC*	*ATCTCCAGGTCAGCCTTGGTCA*
K12	*AGCAGAATCGGAAGGACGCTGA*	*ACCTCGCTCTTGCTGGACTGAA*
K14	*TGCCGAGGAATGGTTCTTCACC*	*GCAGCTCAATCTCCAGGTTCTG*
K15	*AGGACTGACCTGGAGATGCAGA*	*TGCGTCCATCTCCACATTGACC*
K19	*AGCTAGAGGTGAAGATCCGCGA*	*GCAGGACAATCCTGGAGTTCTC*
MEIS1	*AAGCAGTTGGCACAAGACACGG*	*CTGCTCGGTTGGACTGGTCTAT*
MMP9	*GCCACTACTGTGCCTTTGAGTC*	*CCCTCAGAGAATCGCCAGTACT*
MMP10	*TCCAGGCTGTATGAAGGAGAGG*	*GGTAGGCATGAGCCAAACTGTG*
NR2F2	*TGCACGTTGACTCAGCCGAGTA*	*AAGCACACTGAGACTTTTCCTGC*
NOTCH1	*GGTGAACTGCTCTGAGGAGATC*	*GGATTGCAGTCGTCCACGTTGA*
NOTCH3	*TACTGGTAGCCACTGTGAGCAG*	*CAGTTATCACCATTGTAGCCAGG*
ODZ3	*GGACAAGGCTATCACAGTGGAC*	*TTCTGAGGGAGCCGTCATAACC*
PAX6	*TGTCCAACGGATGTGTGAGT*	*TTTCCCAAGCAAAGATGGAC*
PDGFA	*CAGCGACTCCTGGAGATAGACT*	*CGATGCTTCTCTTCCTCCGAATG*
PPARG	*AGCCTGCGAAAGCCTTTTGGTG*	*GGCTTCACATTCAGCAAACCTGG*
PRDM8	*CTGTGTCCTGAGCCATACTTCC*	*CCTTCTGAGGAACCATTTGCTGC*
TGFBI	*AGGACTGACGGAGACCCTCAAC*	*TCCGCTAACCAGGATTTCATCAC*
WNT7A	*TGCCCGGACTCTCATGAAC*	*GTGTGGTCCAGCACGTCTTG*
Gene (Rabbit)	**Forward Primer**	**Reverse Primer**
GAPDH	*GCGAGATCCCGCCAACATCAAGT*	*AGGATGCGTTGCTGACAATC*
PAX6	*GTATTCTTGCTTCAGGTAGAT*	*GAGGCTCAAATGCGACTTCAGCT*
	Primers used for PAX6 transduction	
PAX6 InF	*TTCCCGAATTCTGCAGACCCATGCAGATGCAAAAGTCCAAGTGCTGGACAATCAAAACGTGTCCAACGGATGTG*	
PAX6 InR	*CACATCCGTTGGACACGTTTTGATTGTCCAGCACTTGGACTTTTGCATCTGCATGGGTCTGCAGAATTCGGGAA*	

Extended Data Table 1b. Summary of rabbit transplantation results

	Rabbit number		
GFP-labeled donor cells	**Regeneration and re-epithelization**	**Opaque and vascularized corneal surface**	**Died from systemic infection or unrelated complications**
LSCs	3	0	0
PAX6+ SESCs	5	0	2
shPAX6 LSCs	0	4	1

a, Primer sequences for human and rabbit genes used in this study. **b,** Corneal regeneration and re-epithelization were arrayed three months after transplantation.

Supplementary Material

Refer to Web version on PubMed Central for supplementary material.

Acknowledgments

This study is supported in part by the 973 program (2013CB967504 and 2014CB964900), Project of Fundamental Research Funds (no.2012KF03), State Key laboratory of Ophthalmology, NIH (GM049369), KACST-UCSD Center of Excellence in Nanomedicine, NIH Director's Transformative RO1 Program (R01 EY021374) and CIRM.

References

1. Davanger M, Evensen A. Role of the pericorneal papillary structure in renewal of corneal epithelium. Nature. 1971; 229:560–561. [PubMed: 4925352]
2. Cotsarelis G, Cheng SZ, Dong G, Sun TT, Lavker RM. Existence of slow-cycling limbal epithelial basal cells that can be preferentially stimulated to proliferate: implications on epithelial stem cells. Cell. 1989; 57:201–209. [PubMed: 2702690]
3. Li W, et al. Down-regulation of Pax6 is associated with abnormal differentiation of corneal epithelial cells in severe ocular surface diseases. J Pathol. 2008; 214:114–122. [PubMed: 18027901]
4. Pellegrini G, et al. p63 identifies keratinocyte stem cells. Proc Natl Acad Sci USA. 2001; 98:3156–3161. [PubMed: 11248048]
5. Mills AA, et al. p63 is a p53 homologue required for limb and epidermal morphogenesis. Nature. 1999; 398:708–713. [PubMed: 10227293]
6. Yang A, et al. p63 is essential for regenerative proliferation in limb, craniofacial and epithelial development. Nature. 1999; 398:714–718. [PubMed: 10227294]
7. Koster MI, Kim S, Mills AA, DeMayo FJ, Roop DR. p63 is the molecular switch for initiation of an epithelial stratification program. Genes Dev. 2004; 18:126–131. [PubMed: 14729569]
8. Rama P, et al. Limbal stem-cell therapy and long-term corneal regeneration. N Engl J Med. 2010; 363:147–155. [PubMed: 20573916]
9. Blanpain C, Fuchs E. Epidermal homeostasis: a balancing act of stem cells in the skin. Nature Rev Mol Cell Biol. 2009; 10:207–217. [PubMed: 19209183]
10. Arwert EN, Hoste E, Watt FM. Epithelial stem cells, wound healing and cancer. Nature Rev Cancer. 2012; 12:170–180. [PubMed: 22362215]
11. Kopan R, Fuchs E. A new look into an old problem: keratins as tools to investigate determination, morphogenesis, and differentiation in skin. Genes Dev. 1989; 3:1–15. [PubMed: 2468556]
12. Lauweryns B, van den Oord JJ, Missotten L. The transitional zone between limbus and peripheral cornea. An immunohistochemical study. Invest Ophthalmol Vis Sci. 1993; 34:1991–1999. [PubMed: 8387976]
13. Eichner R, Bonitz P, Sun TT. Classification of epidermal keratins according to their immunoreactivity, isoelectric point, and mode of expression. J Cell Biol. 1984; 98:1388–1396. [PubMed: 6201491]

14. Schlötzer-Schrehardt U, Kruse FE. Identification and characterization of limbal stem cells. Exp Eye Res. 2005; 81:247–264. [PubMed: 16051216]

15. Dorsky RI, Moon RT, Raible DW. Control of neural crest cell fate by the Wnt signalling pathway. Nature. 1998; 396:370–373. [PubMed: 9845073]

16. Eiraku M, et al. Self-organizing optic-cup morphogenesis in three-dimensional culture. Nature. 2011; 472:51–56. [PubMed: 21475194]

17. von Maltzahn J, Bentzinger CF, Rudnicki MA. Wnt7a-Fzd7 signalling directly activates the Akt/mTOR anabolic growth pathway in skeletal muscle. Nature Cell Biol. 2012; 14:186–191. [PubMed: 22179044]

18. Yu FX, et al. Regulation of the Hippo-YAP pathway by G-protein-coupled receptor signaling. Cell. 2012; 150:780–791. [PubMed: 22863277]

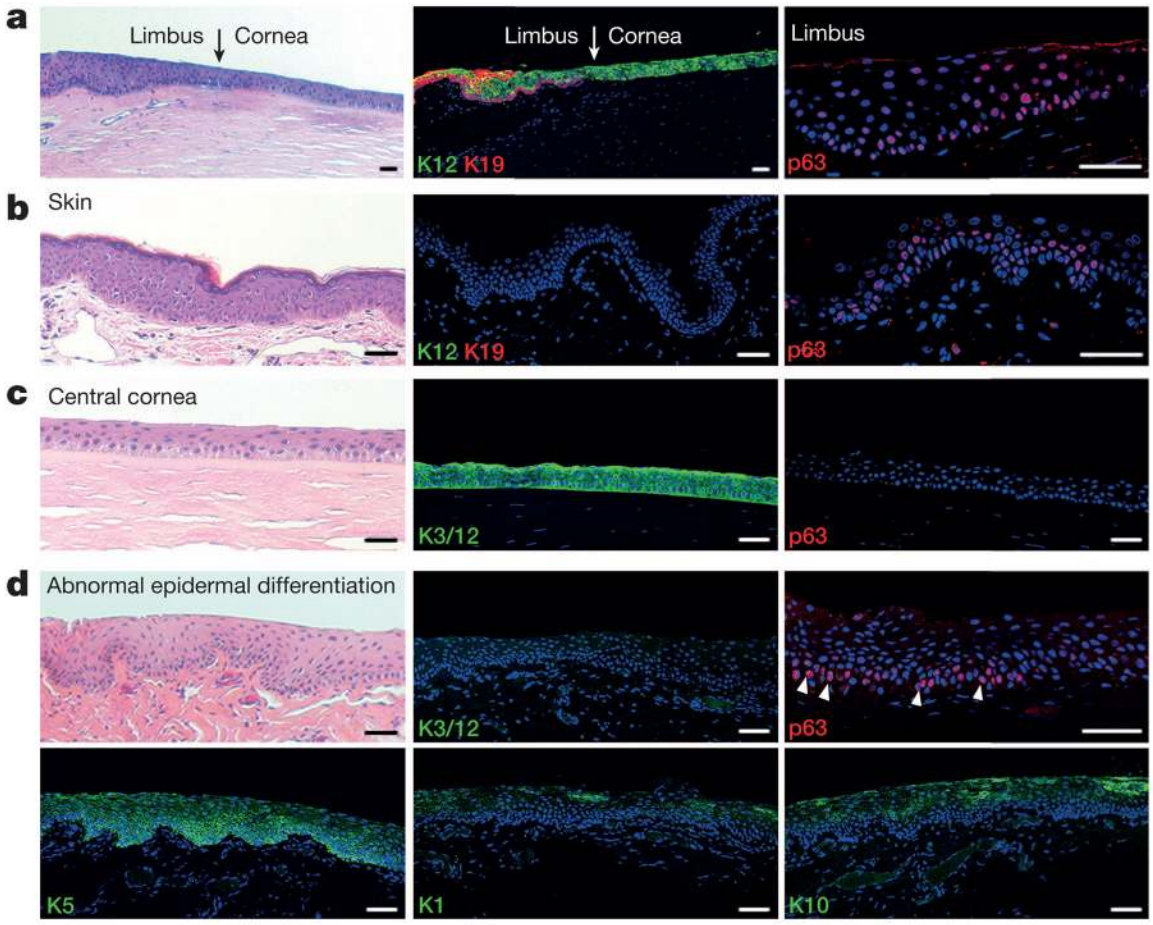

Figure 1. Normal and pathological changes of corneal epithelium, and its comparison to skin

a, Normal cornea–limbus junction (arrows). Limbus identified by K19 and p63 (also see Extended Data Fig. 1e), and cornea by K12. **b**, Normal skin epidermis identified by p63 and K5/K14 (see Extended Data Fig. 1a, b) in the basal layer and absence of K3 and K12 (K3/12). **c**, Normal central cornea labelled by K3/12 and absence of p63 and K1 and K10 (see also Extended Data Fig. 1c, d, f). **d**, Cornea with abnormal epidermal differentiation showing absence of K3/12 (top middle panel) and presence of skin epithelium makers p63 (top right panel) and K5, K1 and K10 (bottom panels). Haematoxylin and eosin (H&E) staining was used for the left panels, with the exception of the bottom left panel. Scale bars, 100 μm.

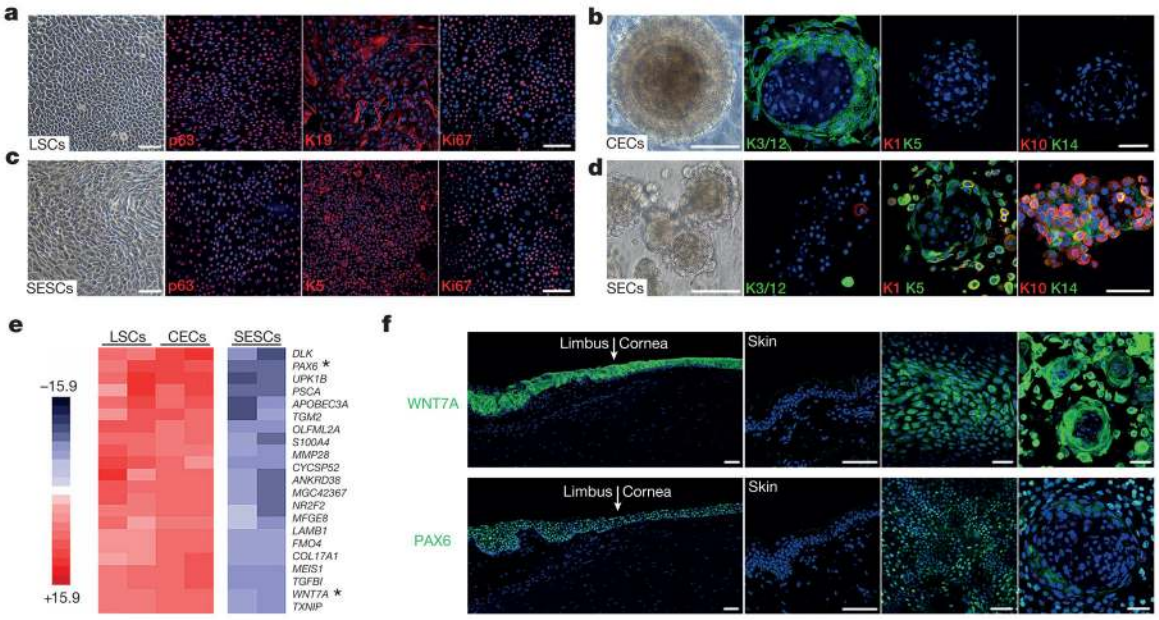

Figure 2. Exclusive expression of WNT7A and PAX6 at limbus and cornea

a–**d**, Immunofluorescence staining of cultured LSCs and SESCs, and three-dimensional differentiated CECs and SECs. Left panels, phase contrast photographs; staining of p63, K19 and Ki67 in LSCs (**a**), p63, K5 and Ki67 in SESCs (**c**), K3/12, K1, K5, K10 and K14 in CECs (**b**) and SECs (**d**) in three-dimensional culture spheres. **e**, Heatmap depicting differential gene expression comparing among LSCs, CECs and SESCs. Asterisks indicate *WNT7A* and *PAX6*. **f**, Immunofluorescence staining of WNT7A and PAX6 at limbus, cornea and skin (left and middle left panels). Expression of WNT7A and PAX6 in cultured LSCs (middle right panels) and three-dimensional CEC spheres (right panels). Scale bars, 100 μm.

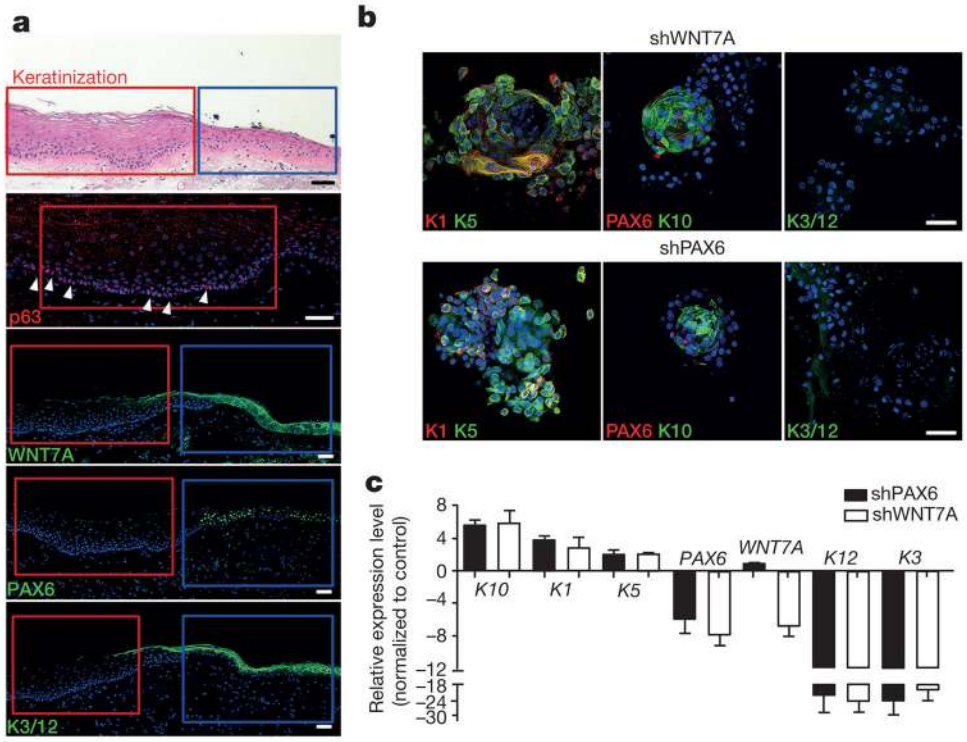

Figure 3. WNT7A and PAX6 are essential for maintenance of cornea cell fate

a, Human corneal epithelium squamous metaplasia. In the top panel, the red box indicates the area of metaplasia and the blue box indicates the area of relatively normal cornea. H&E stain (top panel) shows typical skin epidermal morphology with $p63^{+}$ at basal layer (second panel, arrowheads indicate p63 staining). Loss of WNT7A (middle panel) and PAX6 (fourth panel) was accompanied by absence of corneal K3/12 (bottom panel). Serial sections of the areas marked by red and blue boxes in the top panel are represented in the lower panels. **b**, Immunofluorescence of three-dimensional differentiated cells with *WNT7A* or *PAX6* knockdown; left panels, K1 and K5; middle panels, PAX6 and K10; right panels, K3/12; **c**, Quantitative PCR analysis of gene expression changes of cornea or skin epithelium markers in three-dimensional differentiated cells with *WNT7A* or *PAX6* knockdown (all $n = 3$, $P < 0.05$). Data are shown as means ± s.d. Scale bars, 100 μm.

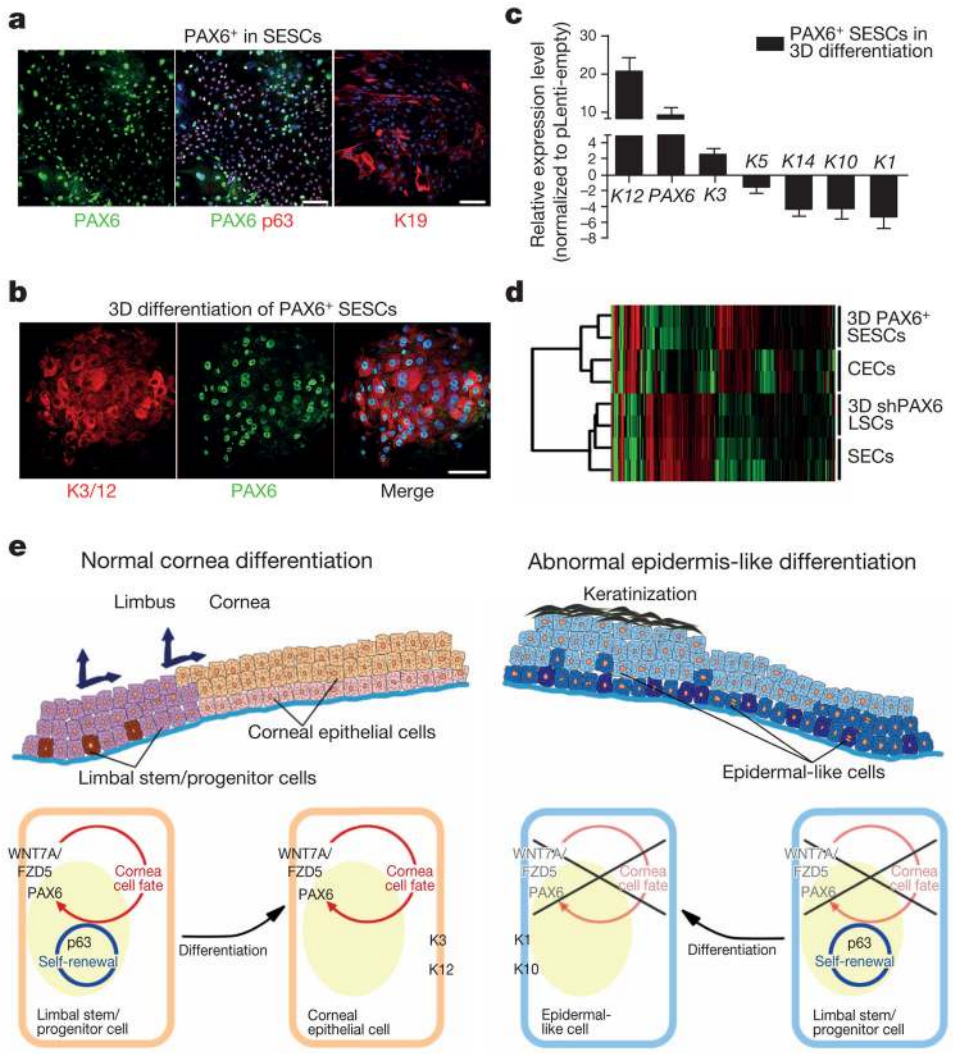

Figure 4. Conversion of SESCs into corneal epithelial-like cells by PAX6 transduction

a, Double immunofluorescence staining of PAX6 and p63 in transfected SESCs, K19 was positive in *PAX6*-transduced (PAX6⁺) SESCs. **b**, Immunofluorescence staining of K3/12 and PAX6⁺ SESCs in three-dimensional (3D) differentiation conditions. **c**, QPCR analysis of gene expression of keratins in PAX6 + SESCs (all $n = 3$, $P < 0.05$). Data are shown as means ± s.d. **d**, Hierarchical cluster analysis among CECs, differentiated LSCs with *PAX6* knockdown (three-dimensional shPAX6 LSCs), SECs and differentiated SESCs with *PAX6* transduction (three-dimensional PAX6⁺ SESCs). **e**, Schematic diagram showing normal LSCs differentiation into CECs (left panel) and proposed mechanism in which loss of WNT7A/PAX6 in LSCs leads to abnormal skin epidermis-like differentiation in corneal surface epithelial cell disease (right panel). Scale bars, 100 μm.

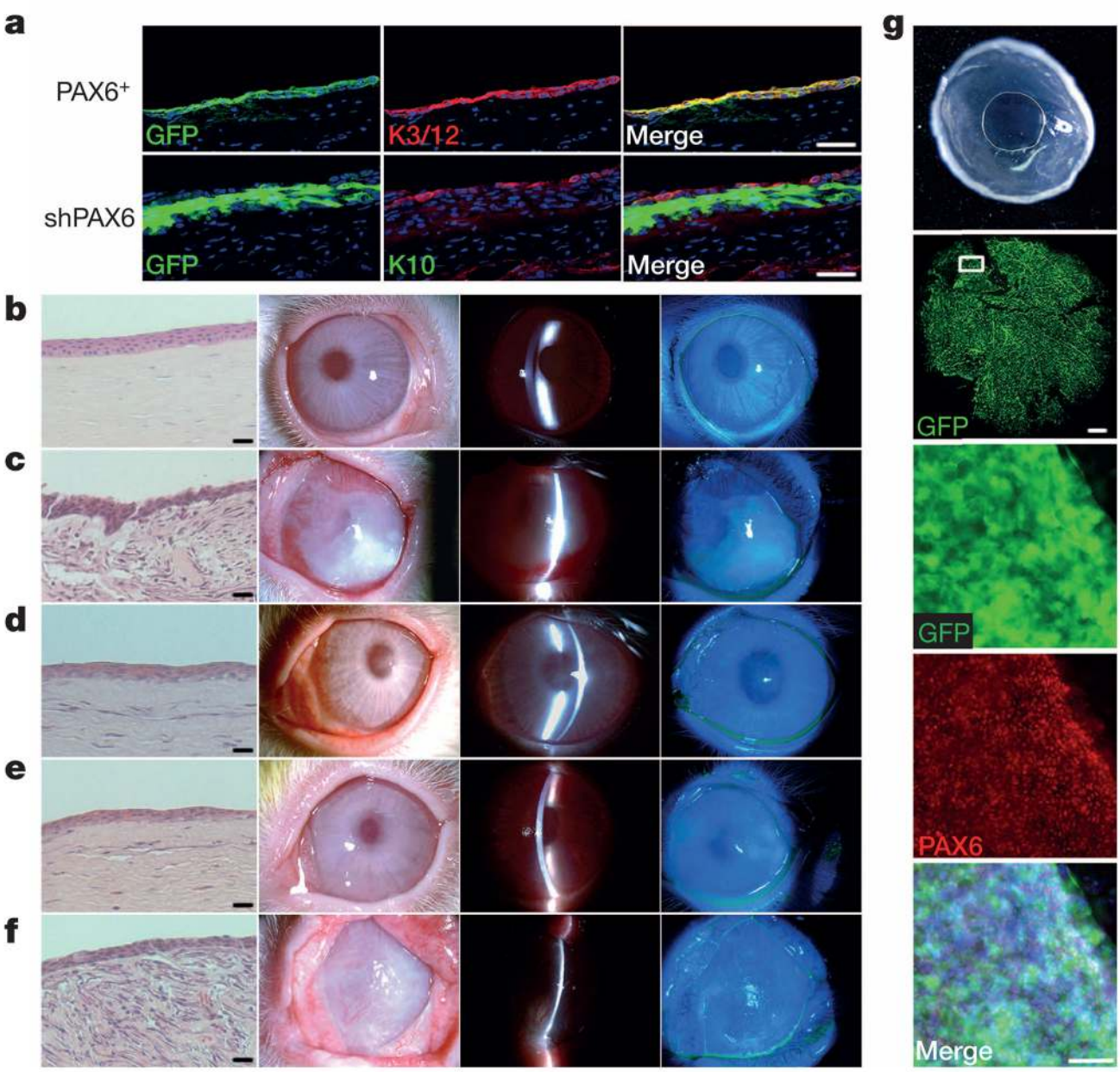

Figure 5. Cell transplantation and cornea epithelium repair in a rabbit limbal stem cell deficiency model

a, Immunofluorescence staining of rabbit corneas 2 months post transplantation. Top panels, cornea transplanted with GFP-labelled PAX6^{+} SESCs, showing positive GFP signals and the expression of the corneal epithelium markers K3 and K12 on the corneal surface. Bottom panels, cornea transplanted with GFP-labelled shPAX6 LSCs, showing positive GFP signals and the expression of the skin epidermal epithelium marker K10. Scale bars, 100 μm. **b–f**, Rabbit corneas 2 months post cell transplantation (left panels, H&E stain; middle two panels, white light micrograph and slit-lamp micrograph; right panels, fluorescein dye staining of corneal epithelium surface). Scale bars, 100 μm. **b**, Normal cornea with typical corneal epithelium histology and intact cornea surface without epithelial defects. **c**, Denuded

cornea covered with a human amniotic membrane only, showing histology of epithelial metaplasia and opaque cornea with vascularization ($n = 4$). **d**, **e**, Cornea transplanted with GFP-labelled LSCs (**d**, $n = 3$) and GFP-labelled PAX6$^+$ SESCs (**e**, $n = 5$), showing corneal epithelium histology, healed and intact cornea surface without epithelial defects. **f**, Cornea transplanted with GFP-labelled, shPAX6-treated LSCs, showing histology of epithelial metaplasia, opaque and vascularized corneal surface with epithelial defects ($n = 4$). **g**, Rabbit cornea 3 months post transplantation with GFP-labelled PAX6$^+$ SESCs: smooth, transparent cornea (top panel) with positive GFP signals (second panel, scale bar, 1 mm). The framed area in the second panel is enlarged to show the expression of PAX6 (middle, fourth and bottom panels, scale bar, 100 μm).